

Study the decays of $\chi_{cJ}(J = 0, 1, 2)$ to light meson pairs with SU(3) flavor symmetry/breaking analysis

Bo Lan¹, Qin-Ze Song¹, Jin-Huan Sheng², Yi Qiao³, and Ru-Min Wang^{1,†}

¹College of Physics and Communication Electronics, Jiangxi Normal University, Nanchang, Jiangxi 330022, China

²School of Physics and Engineering, Henan University of Science and Technology, Luoyang, Henan 471000, China

³College of Physics and Electronic Information, Nanchang Normal University, Nanchang, Jiangxi 330032, China

[†]Corresponding author. Email: ruminwang@sina.com

Based on available experimental results on $\chi_{cJ}(J = 0, 1, 2)$ decays, we investigate the $\chi_{cJ} \rightarrow PP$, VV , PV , and PT decays by using SU(3) flavor symmetry/breaking approach, where P , V , and T denote light pseudoscalar, vector, and tensor mesons, respectively. With the decay amplitude relations determined by SU(3) flavor symmetry/breaking, we present the branching ratios for all $\chi_{cJ} \rightarrow PP$ and $\chi_{cJ} \rightarrow VV$ modes, including ones without experimental data. While theoretical considerations strongly suppress or even forbid most $\chi_{cJ} \rightarrow PV$ and PT decays, we also provide quantitative predictions constrained by existing experimental data. Our results are expected to be accessible in future experiments at BESIII and the planned Super Tau-Charm Facility.

Keywords: charmonium decays, SU(3) symmetry/breaking, light meson pairs

I. INTRODUCTION

The triplet state $\chi_{cJ}(J = 0, 1, 2)$, as the lowest energy P -wave charmonium, has not been widely studied in the past because it cannot be directly obtained from the e^+e^- collisions. However, $\psi(3686)$ provides a clean environment for the production of χ_{cJ} mesons via electromagnetic decays such as $\psi(3686) \rightarrow \gamma\chi_{cJ}$. As the $\psi(3686)$ has been widely studied and collected [1–5], χ_{cJ} decays has obtained more and better measurements, which has led to increased interest in the study of hadronic decays of the χ_{cJ} states [6–12].

The hadronic χ_{cJ} decays have great significance for studying strong force dynamics. On the one hand, the scale of charm quark mass (~ 1.5 GeV) is between the perturbative and non-perturbative QCD in theoretical calculations, it is not large enough for significant heavy quark expansion and not small enough for perturbation theory [13, 14]. On the other hand, most of the hadronic χ_{cJ} decays are suppressed by the Okubo-Zweig-Iizuka (OZI) rule [15]. Moreover, there are still theoretical and experimental discussions regarding the doubly OZI-suppressed decay and singly OZI-suppressed decay mechanisms in some processes [16–20]. Due to these characteristics, understanding hadronic χ_{cJ} decay mechanisms are important for improving theoretical models of both perturbative and non-perturbative QCD, and offer a valuable framework for testing phenomenological models and constraining theoretical parameters.

The χ_{cJ} mesons decay into the two-meson states are particularly useful and they are relatively straightforward to detect and model theoretically. One important feature of charmonium hadronic decays into light mesons is that they are processes rich in gluons. The initial c and \bar{c} quark will annihilate into gluons, which then hadronize to produce the final state of light quarks [21]. Furthermore, the quantum numbers ($I^G J^{PC}$) of mesons produced by two photons and decaying into PP, VV are restricted, they should be 0^+ for isospin and *even*⁺⁺ for parity and charge

conjugation, such as $\chi_{cJ}(J = \text{even})$ mesons. Specifically, due to spin parity conservation, the χ_{c1} cannot decay into two pseudoscalar mesons. And they violate the so-called helicity selection rule, which is defined as $\sigma = (-1)^J P$ [22], and require $\sigma^{\text{initial}} = \sigma_1 \sigma_2$, where J and P are respectively the spin and parity of the particle.

The theoretical calculations of charmonium decays have always been quite difficult, the non-relativistic QCD (NRQCD) framework [23, 24] and phenomenological approaches are suitable and effective to study the charmonium decays. Previous studies of hadronic χ_{cJ} decays used various theoretical frameworks, including parametrization schemes [16, 25], intermediate hadronic loops [18, 26], quark pair creation model with perturbative QCD (pQCD) framework [27], and a description within the effective field theory framework [28], etc. In Refs. [16, 25], parametrization schemes were proposed to further understand the mechanism of violating OZI rules in the two body decays of $\chi_{cJ} \rightarrow PP, VV, SS$, where S denotes scalar meson. These studies suggest that, in addition to singly OZI-suppressed processes, doubly OZI-suppressed processes may play a significant role in the production of isospin-0 light meson pairs, such as $\chi_{c1} \rightarrow f_0 f_0', \omega\omega, \phi\phi, \omega\phi, \eta\eta, \eta\eta'$ and $\eta'\eta'$.

In this paper, we perform a SU(3) flavor symmetry and breaking analysis of charmonium decay processes $\chi_{cJ} \rightarrow PP, VV, PV$, and PT . In Sec. II, the fundamental amplitude relations and theoretical frameworks governing the $\chi_{cJ} \rightarrow PP, VV$ decays are given, and then the numerical results of the $\chi_{cJ} \rightarrow PP, VV$ decays are listed from present experimental data. In Sec. III, corresponding amplitude relations and numerical results of the $\chi_{cJ} \rightarrow PV, PT$ decays are given. The final conclusions can be found in Sec. IV.

II. THE $\chi_{cJ} \rightarrow PP, VV$ DECAYS

A. Amplitude Relations of $\chi_{cJ} \rightarrow PP, VV$

The pseudoscalar and vector meson octet states under the SU(3) flavor symmetry of u, d, s quarks can be written as

$$P = \begin{pmatrix} \frac{\pi^0}{\sqrt{2}} + \frac{\eta_8}{\sqrt{6}} + \frac{\eta_1}{\sqrt{3}} & \pi^+ & K^+ \\ \pi^- & -\frac{\pi^0}{\sqrt{2}} + \frac{\eta_8}{\sqrt{6}} + \frac{\eta_1}{\sqrt{3}} & K^0 \\ K^- & \bar{K}^0 & -\frac{2\eta_8}{\sqrt{6}} + \frac{\eta_1}{\sqrt{3}} \end{pmatrix}, \quad (1)$$

and

$$V = \begin{pmatrix} \frac{\rho^0}{\sqrt{2}} + \frac{\omega_8}{\sqrt{6}} + \frac{\omega_1}{\sqrt{3}} & \rho^+ & K^{*+} \\ \rho^- & -\frac{\rho^0}{\sqrt{2}} + \frac{\omega_8}{\sqrt{6}} + \frac{\omega_1}{\sqrt{3}} & K^{*0} \\ K^{*-} & \bar{K}^{*0} & -\frac{2\omega_8}{\sqrt{6}} + \frac{\omega_1}{\sqrt{3}} \end{pmatrix}, \quad (2)$$

where η_1 - η_8 and ω_1 - ω_8 denote the unmixed states, and according to Particle Data Group (PDG) [29], the mixing of η - η' and ϕ - ω are described as follows.

$$\eta = (\eta_8 \cos \theta_P - \eta_1 \sin \theta_P), \quad (3)$$

$$\eta' = (\eta_8 \sin \theta_P + \eta_1 \cos \theta_P), \quad (4)$$

and

$$\phi = (\omega_8 \cos \theta_V - \omega_1 \sin \theta_V), \quad (5)$$

$$\omega = (\omega_8 \sin \theta_V + \omega_1 \cos \theta_V). \quad (6)$$

Many theoretical works consider the mesons ω and η as pure octet components, experimental observations show that ω and η are actually mixtures of both octet and singlet components, with a specific mixing angle. Therefore, we discuss the branching ratio results that incorporate the η - η' and ϕ - ω mixing with the mixing angle values from the PDG, $\theta_P = [-20^\circ, -10^\circ]$ and $\theta_V = 36.5^\circ$ [29].

As shown in Fig. 1, the singly OZI disconnected and doubly OZI disconnected decay modes are considered. The Fig. 1(a) shows a typical singly OZI process, where gluons produced by initial state annihilation create new quark pairs and undergo quark exchange in the final state. In Fig. 1(b), two quark pairs are created by gluons, and recoil without quark exchanges, which show a doubly OZI process. Based on the SU(3) flavor symmetry, the decay amplitudes of the decay $\chi_{cJ} \rightarrow MM$ can be parameterized as

$$\mathcal{A}^s(\chi_{cJ} \rightarrow M_1 M_2) = a_{1J}^M M_{1j}^i M_{2i}^j + a_{2J}^M M_{1i}^i M_{2j}^j, \quad (7)$$

where $M = P/V$, $i, j = 1, 2, 3$ correspond to the matrix elements in Eqs.(1-2). The a_{1J}^M and a_{2J}^M are non-perturbative coefficients corresponding to the decay modes in Fig. 1(a) and Fig. 1(b), respectively. The specific decay amplitudes for $\chi_{cJ} \rightarrow PP, VV$ with the SU(3) flavor symmetry are listed in the second column of Tab. I.

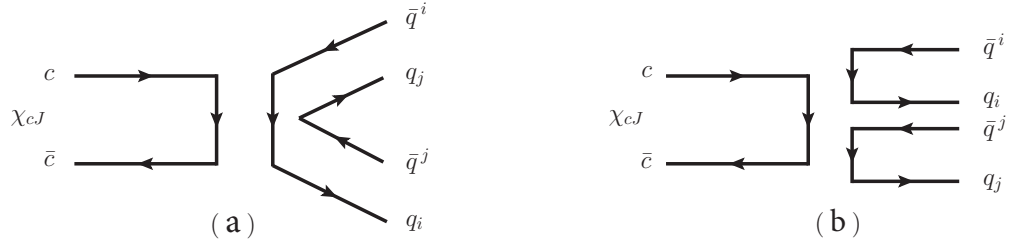


FIG. 1: The singly OZI disconnected (a) and doubly OZI disconnected (b) diagrams of the $\chi_{cJ} \rightarrow MM$ decays.

The SU(3) flavor symmetry assumes that u , d , and s quarks have equal masses. SU(3) flavor symmetry breaking is given by the current quark mass term in the QCD Lagrangian with $m_{u,d} \ll m_s$ in the Standard Model. In order to achieve a more accurate analysis, we take into account the symmetry breaking. The diagonalized mass matrix can be expressed as [30–32]

$$\begin{pmatrix} m_u & 0 & 0 \\ 0 & m_d & 0 \\ 0 & 0 & m_s \end{pmatrix} = \frac{1}{3}(m_u + m_d + m_s)I + \frac{1}{2}(m_u - m_d)X + \frac{1}{6}(m_u + m_d - 2m_s)W, \quad (8)$$

where I is the identity matrix, and X and W represented as

$$X = \begin{pmatrix} 1 & 0 & 0 \\ 0 & -1 & 0 \\ 0 & 0 & 0 \end{pmatrix}, \quad W = \begin{pmatrix} 1 & 0 & 0 \\ 0 & 1 & 0 \\ 0 & 0 & -2 \end{pmatrix}. \quad (9)$$

Considering the mass difference between the s quark and the u, d quarks, the W part of the diagonalized mass matrix to account for symmetry breaking is included. Thus, the amplitude of the breaking part can be written as

$$\mathcal{A}^b(\chi_{cJ} \rightarrow M_1 M_2) = b_J^M M_{1j}^i W_k^j M_{2i}^k, \quad (10)$$

TABLE I: The SU(3) symmetry and breaking amplitudes of $\chi_{cJ} \rightarrow P_1 P_2$ and $\chi_{cJ} \rightarrow V_1 V_2$.

Decay modes	Symmetry amplitudes	Breaking amplitudes
$\chi_{cJ} \rightarrow \pi^+ \pi^- / \rho^+ \rho^-$	$2a_{1J}^M$	$2b_J^M$
$\chi_{cJ} \rightarrow K^+ K^- / K^{*+} K^{*-}$	$2a_{1J}^M$	$-b_J^M$
$\chi_{cJ} \rightarrow K^0 \bar{K}^0 / K^{*0} \bar{K}^{*0}$	$2a_{1J}^M$	$-b_J^M$
$\chi_{cJ} \rightarrow \pi^0 \pi^0 / \rho^0 \rho^0$	$\sqrt{2}a_{1J}^M$	$\sqrt{2}b_J^M$
$\chi_{cJ} \rightarrow \eta_1 \eta_1 / \omega_1 \omega_1$	$\sqrt{2}(a_{1J}^M + 3a_{2J}^M)$	0
$\chi_{cJ} \rightarrow \eta_1 \eta_8 / \omega_1 \omega_8$	0	$2\sqrt{2}b_J^M$
$\chi_{cJ} \rightarrow \eta_8 \eta_8 / \omega_8 \omega_8$	$\sqrt{2}a_{1J}^M$	$-\sqrt{2}b_J^M$
$\chi_{cJ} \rightarrow \eta \eta / \phi \phi$	$\sqrt{2}a_{1J}^M + \frac{3\sqrt{2}}{2}a_{2J}^M(1 - \cos 2\theta_M)$	$-\sqrt{2}b_J^M \cos \theta_M(4 \sin \theta_M + \cos \theta_M)$
$\chi_{cJ} \rightarrow \eta \eta' / \phi \omega$	$-\frac{3\sqrt{2}}{2}a_{2J}^M \sin 2\theta_M$	$\sqrt{2}b_J^M(2 \cos 2\theta_M - \frac{1}{2} \sin 2\theta_M)$
$\chi_{cJ} \rightarrow \eta' \eta' / \omega \omega$	$\sqrt{2}a_{1J}^M + \frac{3\sqrt{2}}{2}a_{2J}^M(1 + \cos 2\theta_M)$	$\sqrt{2}b_J^M \sin \theta_M(4 \cos \theta_M - \sin \theta_M)$

where b_J^M is the non-perturbative coefficient of the breaking term. The decay amplitudes for $\chi_{cJ} \rightarrow P_1 P_2, V_1 V_2$ with SU(3) breaking are given in the third column of Tab. I, and it is worth noting that the minus signs of the breaking terms are from the mathematical structure of the W matrix given in Eq. (9). Furthermore, we follow Ref. [33, 34] to make a similar convention regarding the final state being identical particles, where the amplitude of the final state of identical particles is multiplied by a coefficient with $\sqrt{2}$.

In general, the involved three parameters ($a_{1J}^M, a_{2J}^M, b_J^M$) are complex. Since an overall phase can be removed without losing generality, we set a_{1J}^M to be real, then there are five real independent parameters are considered in data analysis

$$a_{1J}^M, \quad a_{2J}^M e^{i\alpha_{JM}}, \quad b_J^M e^{i\beta_{JM}}. \quad (11)$$

Where α_{JM} is the relative phase between a_{1J}^M and a_{2J}^M , and β_{JM} is the relative phase between a_{1J}^M and b_J^M . It should be noted that when only one decay mode is contributed, the relative phase does not appear, and its own phase disappears in the form of modulus in the branching ratio calculations, so there is no need for special definition. The numerical results of branching ratio are provided by Monte Carlo simulation method, and all experimental inputs are from PDG [29]. Each process inputs a large number of random samples to ensure that the distribution of numerical results consists of at least 10000 sets of valid results. More detailed discussions will be provided in the following contents. The branching ratio is calculated using the fundamental two-body decay formula, which can be expressed

as

$$\mathcal{B}(\chi_{cJ} \rightarrow M_1 M_2) = \frac{|\vec{p}|}{8\pi M_{\chi_{cJ}}^2 \Gamma_{\chi_{cJ}}} \left| \mathcal{A}(\chi_{cJ} \rightarrow M_1 M_2) \right|^2, \quad (12)$$

where $\Gamma_{\chi_{cJ}}$ is the decay width of the χ_{cJ} meson, and the center-of-mass momentum $|\vec{p}| \equiv \frac{\sqrt{[M_{\chi_{cJ}}^2 - (m_{M_1} + m_{M_2})^2][M_{\chi_{cJ}}^2 - (m_{M_1} - m_{M_2})^2]}}{2M_{\chi_{cJ}}}$.

B. Numerical results of the $\chi_{cJ} \rightarrow PP$ decays

Numerical results of the $\chi_{cJ} \rightarrow PP$ decays will be given in this section. The experimental branching ratios are provided in the second column in Tab. II for χ_{c0} decays and Tab. III for χ_{c2} decays from PDG [29]. Based on SU(3) symmetry and breaking amplitudes, we have obtained and analyzed two sets of branching ratio results for $\chi_{cJ} \rightarrow PP$ decays. The results considering SU(3) symmetry are shown in the third column of Tab. II and Tab. III, while those incorporating breaking effects are listed in the fourth columns. Furthermore, the decays of χ_{c1} ($J^{PC} = 1^{++}$) into two pseudoscalar mesons is forbidden by spin-parity conservation and helicity selection rule, therefore, they are not considered in this analysis.

Firstly, analyze the results within the SU(3) flavor symmetry. The experimental data of the $\chi_{c0} \rightarrow K^+ K^-$, $\eta\eta, \eta\eta', \eta'\eta'$ and $\chi_{c2} \rightarrow K^+ K^-, \eta\eta, \eta\eta', \eta'\eta'$ decays can be explained within 1σ error. After using the constrained non-perturbative parameters from the data of $\chi_{c0} \rightarrow K^+ K^-, \eta\eta, \eta\eta', \eta'\eta'$ or $\chi_{c2} \rightarrow K^+ K^-, \eta\eta, \eta\eta', \eta'\eta'$ decays, the predicted branching ratios of the $\chi_{c0} \rightarrow \pi\pi$ and $\chi_{c2} \rightarrow \pi\pi$ decays slightly deviate their experimental data within 1σ error, nevertheless, they could be consistent within about 2σ or 3σ error bars. All predicted branching ratios also falling within a relatively accurate range. This suggests that the SU(3) flavor symmetry exhibits good conformity with the overall decay modes. In particular, the a_{1J}^P term exhibits dominance across most decay channels. The maximum value of the ratio $\frac{a_{2J}^P}{a_{1J}^P}$ reach 37% for the χ_{c0} decays and 45% for the χ_{c2} decays, and they are supported by suppressed from doubly OZI [35, 36]. Within SU(3) flavor symmetry, amplitude form of $\eta\eta'$ only has a_{2J}^P component, which also conforms to the result of suppression.

After considering the SU(3) flavor breaking effects, as listed in the fourth columns of Tab. II and Tab. III, all experimental data of both χ_{c0} and χ_{c2} decays including the $\pi\pi$ modes, can be explained within 1σ error bar. In terms of the ratio $\frac{b_J^M}{a_{1J}^M}$ as the breaking ratio, the maximum value is 14% in the χ_{c0} decays and 22% in the χ_{c2} decays. Although b_J^M term contributions are small compared to the a_{2J}^P , they provide better fits for the relative experimental data within 1σ error. As a result, there is an increased error range for certain channels, such as $\chi_{c2} \rightarrow K^+ K^-$ and $\chi_{c2} \rightarrow K^0 \bar{K}^0$. It implies that while the breaking contributions are small, they should not be ignored.

For the non-perturbative parameters $a_{1J}^P, a_{2J}^P, b_J^P, |\alpha_{JP}|$ and $|\beta_{JP}|$, their allowed ranges are listed in the last five lines of Tab. II and Tab. III. Please note that their allowed values are interrelated. Their interrelations are shown in Fig. 2.

Noted that the recent measurements on BESIII [37] report precision branching ratios

$$\begin{aligned} \mathcal{B}(\chi_{c0} \rightarrow K^+ K^-) &= (6.36 \pm 0.15) \times 10^{-3}, & \mathcal{B}(\chi_{c0} \rightarrow \pi^+ \pi^-) &= (6.06 \pm 0.15) \times 10^{-3}, \\ \mathcal{B}(\chi_{c2} \rightarrow K^+ K^-) &= (1.22 \pm 0.03) \times 10^{-3}, & \mathcal{B}(\chi_{c2} \rightarrow \pi^+ \pi^-) &= (1.61 \pm 0.04) \times 10^{-3}, \end{aligned}$$

TABLE II: The branching ratios for the $\chi_{c0} \rightarrow PP$ decays within 1σ error (in units of 10^{-3}). # indicates that experimental data was not used to derive the numerical results.

	Exp. data [29]	Symmetry	Including breaking
$\mathcal{B}(\chi_{c0} \rightarrow \pi^+\pi^-)$...	6.33 ± 0.33	5.67 ± 0.27
$\mathcal{B}(\chi_{c0} \rightarrow \pi^0\pi^0)$...	3.17 ± 0.16	2.83 ± 0.13
$\mathcal{B}(\chi_{c0} \rightarrow \pi\pi)$	8.50 ± 0.40	$9.50 \pm 0.49^\#$	8.50 ± 0.40
$\mathcal{B}(\chi_{c0} \rightarrow K^+K^-)$	6.07 ± 0.33	6.08 ± 0.32	6.07 ± 0.33
$\mathcal{B}(\chi_{c0} \rightarrow K^0\bar{K}^0)$...	6.08 ± 0.32	6.07 ± 0.33
$\mathcal{B}(\chi_{c0} \rightarrow K\bar{K})$...	12.16 ± 0.63	12.14 ± 0.66
$\mathcal{B}(\chi_{c0} \rightarrow \eta\eta)$	3.01 ± 0.25	2.91 ± 0.15	2.92 ± 0.16
$\mathcal{B}(\chi_{c0} \rightarrow \eta\eta')$	0.09 ± 0.01	0.09 ± 0.01	0.09 ± 0.01
$\mathcal{B}(\chi_{c0} \rightarrow \eta'\eta')$	2.17 ± 0.12	2.17 ± 0.12	2.17 ± 0.12
$a_{10}^P (10^{-2})$...	5.41 ± 0.28	5.30 ± 0.27
$a_{20}^P (10^{-2})$...	1.48 ± 0.56	1.12 ± 1.04
$b_0^P (10^{-2})$	0.40 ± 0.35
$ \alpha_{0P} $...	$(119.75 \pm 9.74)^\circ$	$(142.09 \pm 37.82)^\circ$
$ \beta_{0P} $	$(136.36 \pm 43.54)^\circ$

TABLE III: The branching ratios for the $\chi_{c2} \rightarrow PP$ decays within 1σ error (in units of 10^{-4}). # indicates that experimental data was not used to derive the numerical results.

	Exp. data [29]	Symmetry	Including breaking
$\mathcal{B}(\chi_{c2} \rightarrow \pi^+\pi^-)$...	11.67 ± 0.47	15.13 ± 0.67
$\mathcal{B}(\chi_{c2} \rightarrow \pi^0\pi^0)$...	5.83 ± 0.24	7.57 ± 0.33
$\mathcal{B}(\chi_{c2} \rightarrow \pi\pi)$	22.70 ± 1.00	$17.50 \pm 0.71^\#$	22.70 ± 1.00
$\mathcal{B}(\chi_{c2} \rightarrow K^+K^-)$	10.20 ± 1.50	11.24 ± 0.46	10.20 ± 1.50
$\mathcal{B}(\chi_{c2} \rightarrow K^0\bar{K}^0)$...	11.24 ± 0.46	10.20 ± 1.50
$\mathcal{B}(\chi_{c2} \rightarrow K\bar{K})$...	22.48 ± 0.91	20.39 ± 3.00
$\mathcal{B}(\chi_{c2} \rightarrow \eta\eta)$	5.50 ± 0.50	5.22 ± 0.22	5.42 ± 0.42
$\mathcal{B}(\chi_{c2} \rightarrow \eta\eta')$	0.22 ± 0.05	0.22 ± 0.05	0.22 ± 0.05
$\mathcal{B}(\chi_{c2} \rightarrow \eta'\eta')$	0.46 ± 0.06	0.46 ± 0.06	0.46 ± 0.06
$a_{12}^P (10^{-2})$...	1.02 ± 0.04	1.03 ± 0.08
$a_{22}^P (10^{-2})$...	0.35 ± 0.11	0.32 ± 0.16
$b_2^P (10^{-2})$	0.14 ± 0.08
$ \alpha_{2P} $...	$(170.17 \pm 9.74)^\circ$	$(165.58 \pm 14.32)^\circ$
$ \beta_{2P} $	$(31.51 \pm 30.94)^\circ$

which are not used to constrain the non-perturbative coefficients and to predict the not-yet-measured branching ratios in this work. Our predictions of $\mathcal{B}(\chi_{c0,2} \rightarrow \pi^+\pi^-)$ are consistent with above data within 1σ error bar. Above experimental data of $\mathcal{B}(\chi_{c0} \rightarrow K^+K^-)$ or $\mathcal{B}(\chi_{c2} \rightarrow K^+K^-)$ are consistent with ones from PDG [29] within 1σ or 1.2σ error bar(s).

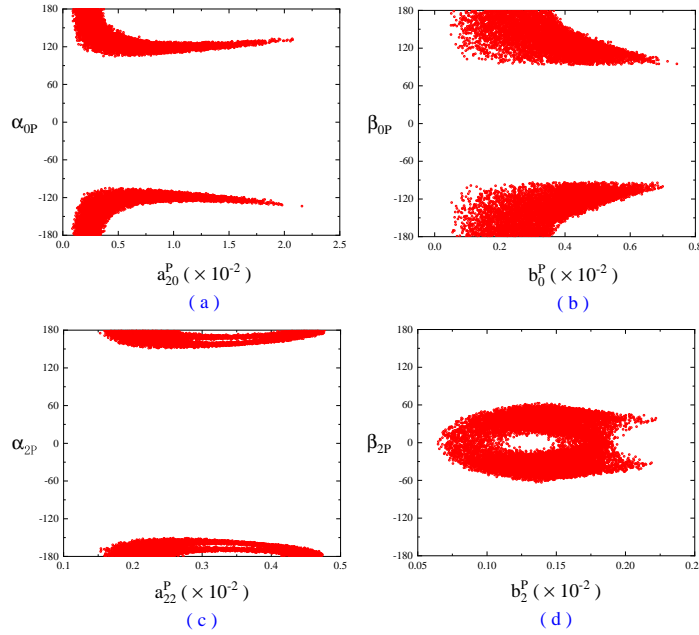


FIG. 2: The parameter correlations in the $\chi_{c0,2} \rightarrow PP$ decays.

In previous studies, several results provide useful reference points. For instance, Ref. [16] proposed parametrization schemes to further understand the mechanisms that violate the OZI rule. Their work deepened the understanding of charmonium decays mechanisms by defining the relative strength r and some other physical quantities based on the SU(3) flavor approach. They provided good fit results based on experimental data at the time, and provide useful insights into the channels of the isospin-0 light meson pairs. With the update of experimental measurements, we have provided more theoretical predictions under the SU(3) flavor approach using the latest experimental data. Our predicted results are expected to contribute to future research on $\chi_{cJ} \rightarrow PP$ decays.

C. Numerical results of $\chi_{cJ} \rightarrow VV$

For $\chi_{cJ} \rightarrow VV$ decays, they are similar to PP channels, but with some key differences. The $\chi_{c1} \rightarrow VV$ decays are suppressed compared to $\chi_{c0,2} \rightarrow VV$ decays since they violate helicity selection rule [22], much like their PP channels. However, interestingly, $\chi_{c1} \rightarrow VV$ decays are not forbidden as initially expected. As experimental data has accumulated, increasing observations have revealed significant discrepancies between the data and the predictions based on the selection rule. One possible reason for the failure of the perturbative approach here could be that, although the charm quark is relatively heavy, it does not meet the mass threshold required by pQCD [26]. This suggests that there might be other mechanisms at play, such as higher-order contributions, final-state interactions, or long-distance effects, that could contribute to processes typically forbidden by the helicity selection rule. In any case, we present the branching ratio results for $\chi_{c0,1,2} \rightarrow VV$ based on the SU(3) flavor symmetry/breaking in this section.

The experimental data are given in the second columns of Tab. IV, Tab. V and Tab. VI for the $\chi_{c0} \rightarrow VV$, $\chi_{c1} \rightarrow VV$ and $\chi_{c2} \rightarrow VV$ decays, respectively. Our branching ratio predictions based on SU(3) flavor symmetry

TABLE IV: The branching ratios for the $\chi_{c0} \rightarrow VV$ decays within 1σ error (in units of 10^{-3}).

	Exp. data [29]	Symmetry	Including breaking
$\mathcal{B}(\chi_{c0} \rightarrow \rho^+ \rho^-)$...	2.04 ± 0.37	2.28 ± 1.56
$\mathcal{B}(\chi_{c0} \rightarrow \rho^0 \rho^0)$...	1.02 ± 0.18	1.14 ± 0.78
$\mathcal{B}(\chi_{c0} \rightarrow \rho \rho)$...	3.06 ± 0.55	3.42 ± 2.33
$\mathcal{B}(\chi_{c0} \rightarrow K^{*+} K^{*-})$...	1.95 ± 0.35	1.70 ± 0.60
$\mathcal{B}(\chi_{c0} \rightarrow K^{*0} \bar{K}^{*0})$	1.70 ± 0.60	1.95 ± 0.35	1.70 ± 0.60
$\mathcal{B}(\chi_{c0} \rightarrow K^* \bar{K}^*)$...	3.90 ± 0.70	3.40 ± 1.20
$\mathcal{B}(\chi_{c0} \rightarrow \phi \phi)$	0.848 ± 0.031	0.85 ± 0.03	0.85 ± 0.03
$\mathcal{B}(\chi_{c0} \rightarrow \phi \omega)$	0.142 ± 0.013	0.142 ± 0.013	0.142 ± 0.013
$\mathcal{B}(\chi_{c0} \rightarrow \omega \omega)$	0.97 ± 0.11	0.97 ± 0.11	0.97 ± 0.11
$a_{10}^V (10^{-2})$...	3.24 ± 0.37	2.98 ± 0.85
$a_{20}^V (10^{-2})$...	0.86 ± 0.06	0.85 ± 0.14
$b_0^V (10^{-2})$	0.78 ± 0.78
$ \alpha_{0V} $...	$(106.57 \pm 16.04)^\circ$	$(120.89 \pm 59.01)^\circ$
$ \beta_{0V} $	$(90.00 \pm 90.00)^\circ$

TABLE V: The branching ratios for the $\chi_{c1} \rightarrow VV$ decays within 1σ error (in units of 10^{-4}). # indicates that experimental data was not used to derive the numerical results.

	Exp. data [29]	Symmetry	Including breaking
$\mathcal{B}(\chi_{c1} \rightarrow \rho^+ \rho^-)$...	12.35 ± 1.92	15.18 ± 4.96
$\mathcal{B}(\chi_{c1} \rightarrow \rho^0 \rho^0)$...	6.17 ± 0.96	7.59 ± 2.48
$\mathcal{B}(\chi_{c1} \rightarrow \rho \rho)$...	18.52 ± 2.87	22.77 ± 7.43
$\mathcal{B}(\chi_{c1} \rightarrow K^{*+} K^{*-})$...	11.85 ± 1.84	13.22 ± 3.21
$\mathcal{B}(\chi_{c1} \rightarrow K^{*0} \bar{K}^{*0})$	14.00 ± 4.00	11.84 ± 1.84	13.20 ± 3.20
$\mathcal{B}(\chi_{c1} \rightarrow K^* \bar{K}^*)$...	23.69 ± 3.68	26.42 ± 6.41
$\mathcal{B}(\chi_{c1} \rightarrow \phi \phi)$	4.26 ± 0.21	$5.24 \pm 0.73^\#$	4.26 ± 0.21
$\mathcal{B}(\chi_{c1} \rightarrow \phi \omega)$	0.27 ± 0.04	0.27 ± 0.04	0.27 ± 0.04
$\mathcal{B}(\chi_{c1} \rightarrow \omega \omega)$	5.70 ± 0.70	5.70 ± 0.70	5.70 ± 0.70
$a_{11}^V (10^{-3})$...	6.96 ± 0.54	7.59 ± 1.17
$a_{21}^V (10^{-3})$...	1.06 ± 0.10	1.05 ± 0.19
$b_1^V (10^{-3})$	1.17 ± 1.14
$ \alpha_{1V} $...	$(105.42 \pm 28.65)^\circ$	$(134.65 \pm 45.26)^\circ$
$ \beta_{1V} $	$(47.56 \pm 47.56)^\circ$

are listed in the third columns of these tables, while predictions including breaking effects are displayed in the fourth columns.

The results of $\chi_{c0} \rightarrow VV$ with the SU(3) flavor symmetry show good agreement with present experimental data within 1σ error, and their error ranges are small. However, for $\chi_{c1} \rightarrow VV$ decays, the constrained a_{11}^V from $\chi_{c1} \rightarrow K^{*0} \bar{K}^{*0}, \phi \omega, \omega \omega$ can not explain the data of $\chi_{c1} \rightarrow \phi \phi$ within 1σ error, nevertheless, one parameter a_{11}^V could explain

TABLE VI: The branching ratios for the $\chi_{c2} \rightarrow VV$ decays within 1σ error (in units of 10^{-4}). $^\#$ indicates that experimental data was not used to derive the numerical results.

	Exp. data [29]	Symmetry	Including breaking
$\mathcal{B}(\chi_{c2} \rightarrow \rho^+ \rho^-)$	\dots	27.08 ± 5.20	18.38 ± 8.04
$\mathcal{B}(\chi_{c2} \rightarrow \rho^0 \rho^0)$	\dots	13.54 ± 2.60	9.19 ± 4.02
$\mathcal{B}(\chi_{c2} \rightarrow \rho \rho)$	\dots	40.62 ± 7.80	27.57 ± 12.06
$\mathcal{B}(\chi_{c2} \rightarrow K^{*+} K^{*-})$	\dots	26.04 ± 5.00	20.39 ± 7.37
$\mathcal{B}(\chi_{c2} \rightarrow K^{*0} \bar{K}^{*0})$	22.00 ± 9.00	26.00 ± 4.99	20.36 ± 7.36
$\mathcal{B}(\chi_{c2} \rightarrow K^* \bar{K}^*)$	\dots	52.03 ± 9.99	40.76 ± 14.74
$\mathcal{B}(\chi_{c2} \rightarrow \phi \phi)$	12.30 ± 0.70	12.30 ± 0.70	12.30 ± 0.70
$\mathcal{B}(\chi_{c2} \rightarrow \phi \omega)$	0.097 ± 0.028	0.097 ± 0.028	0.097 ± 0.028
$\mathcal{B}(\chi_{c2} \rightarrow \omega \omega)$	8.60 ± 1.00	$13.57 \pm 2.36^\#$	8.60 ± 1.00
$a_{12}^V (10^{-3})$	\dots	16.31 ± 1.87	13.73 ± 3.09
$a_{22}^V (10^{-3})$	\dots	0.98 ± 0.17	0.98 ± 0.48
$b_2^V (10^{-3})$	\dots	\dots	2.92 ± 2.59
$ \alpha_{2V} $	\dots	$(90.00 \pm 90.00)^\circ$	$(90.00 \pm 90.00)^\circ$
$ \beta_{2V} $	\dots	\dots	$(131.21 \pm 48.70)^\circ$

all four data if the error expand from 1σ to 1.1σ errors. As for $\chi_{c2} \rightarrow VV$ decays, all four experimental data can be explained by one parameter a_{22}^V within 1.5σ errors. The maximum values of $\frac{a_{22}^V}{a_{1J}^V}$ across all datasets reach 30% for the χ_{c0} decays, 17% for the χ_{c1} decays, and 8% for the χ_{c2} decays. They indicate the dominant role of the a_{1J}^V amplitudes in the $\chi_{cJ} \rightarrow VV$ decays. Despite some theoretical shortcomings, the SU(3) flavor symmetry captures the essential correlations and still offers reasonable predictions. Thus, the results based on the SU(3) flavor symmetry reflect universal trends, with a small uncertainty in the data distribution, offering useful reference values.

Now turn to the results including the SU(3) flavor breaking terms. All present experimental data of the $\chi_{c0,1,2} \rightarrow VV$ decays can be explained within 1σ error bar if including the SU(3) flavor breaking terms. The maximum ratio of breaking contributions, i.e. $\frac{b_J^V}{a_{1J}^V}$, is 55% for the χ_{c0} decays, 33% for the χ_{c1} decays, and 48% for the χ_{c2} decays. Compared to the $\chi_{cJ} \rightarrow PP$ decays, the allowed breaking contributions for χ_{c0} and χ_{c2} are more significant in the VV decays at present, and they notably alter the distribution of branching ratios. The fundamental reason is that there are five relevant non-perturbative parameters and only four experimental data in the $\chi_{c0/c1/c2} \rightarrow VV$ decays, and the four experimental data are not enough to constrain on the five parameters. So b_J^V and β_{JV} are not well determined due to the lack of experimental values for the $\rho\rho$ channels, making it difficult to accurately predict the contribution of the breaking. And in the decays of $\chi_{c2} \rightarrow VV$, the constraints on parameters are further weakened due to the large error of the $K^{*0} \bar{K}^{*0}$ channel, such as a_{22}^V and α_{2V} . Therefore, as the breaking contributions are included, the uncertainty in the predicted results also becomes larger, especially for some decay channels like $\chi_{c0,1,2} \rightarrow \rho\rho$ and $\chi_{c1,2} \rightarrow K^* \bar{K}^*$. However, the $\phi\phi$, $\phi\omega$, and $\omega\omega$ channels with good agreement still offer valuable insights, the predicted

results reflect the basic distribution range, provide early useful reference points. Under same approach, the error ranges will decrease with more experimental inputs in the future.

Fig. 3 shows the relationship between the constrained symmetry/breaking parameters (a_{2J}^V, b_J^V) and they their associated phases (α_{JV}, β_{JV}). One can see that, after satisfying all relevant experimental data, the allowed spaces are still large. This may indicate that the non-perturbative coefficients have not been very well limited by present experimental data within 1σ error, further leading to an increase in the uncertainty range of some predicted branching ratio results.

Now we discuss the non-yet-measured $\chi_{cJ} \rightarrow \rho\rho$ decays. Previous works given that $\mathcal{B}(\chi_{c0} \rightarrow \rho\rho) = (1.88 \pm 1.80) \times 10^{-3}$ and $\mathcal{B}(\chi_{c2} \rightarrow \rho\rho) = (2.41 \pm 2.22) \times 10^{-3}$ in a general factorization scheme [25], and $\mathcal{B}(\chi_{c1} \rightarrow \rho\rho)$ lies in $[26, 54] \times 10^{-4}$ by the intermediate meson loop contributions [26]. Our predictions are consistent with them, and our ones of the $\chi_{c1,2} \rightarrow \rho\rho$ decays are relatively more precise ranges.

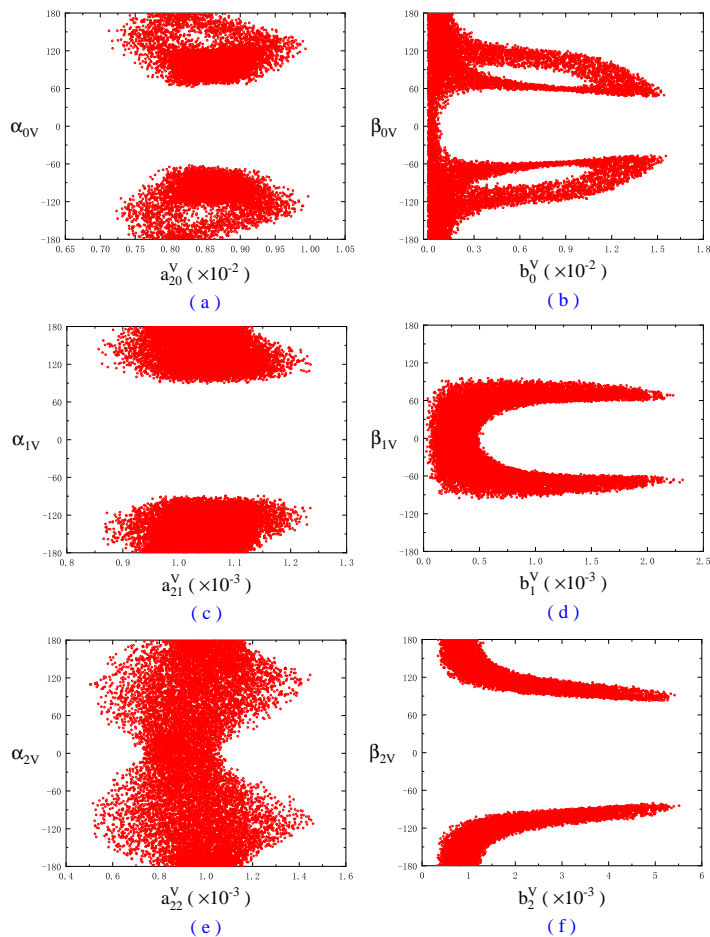


FIG. 3: The parameter correlations in the $\chi_{c0,1,2} \rightarrow VV$ decays.

III. THE $\chi_{cJ} \rightarrow PV, PT$ DECAYS

A. Amplitude relations of the $\chi_{cJ} \rightarrow PV$ and PT decays

The decays of $\chi_{c0,2} \rightarrow PV$ and PT are suppressed by helicity selection rule, furthermore, the G-parity or isospin conservation exists in these decays. Rendering conventional theoretical approaches are significantly challenged in addressing these suppressed decay modes. Due to the helicity selection rule, no many $\chi_{cJ} \rightarrow PV, PT$ decay channels have been measured. The decay of $\chi_{c0} \rightarrow PV$ and PT are vanish due to charmed vector current conservation and parity conservation forbidden by spin-parity conservation [38], and lack the robust phenomenological constraints in the absence of experimental observable values [38, 39]. Therefore, only the χ_{c1} and χ_{c2} decays will be discussed in this section.

The SU(3) flavor symmetry/breaking approach is still used to obtain the branching ratio results of $\chi_{cJ} \rightarrow PV$ and PT . The tensor meson octet states can be written as

$$T = \begin{pmatrix} \frac{a_2^0}{\sqrt{2}} + \frac{f_2^8}{\sqrt{6}} + \frac{f_2^0}{\sqrt{3}} & a_2^+ & K_2^{*+} \\ a_2^- & -\frac{a_2^0}{\sqrt{2}} + \frac{f_2^8}{\sqrt{6}} + \frac{f_2^0}{\sqrt{3}} & K_2^{*0} \\ K_2^{*-} & \bar{K}_2^{*0} & -\frac{2f_2^8}{\sqrt{6}} + \frac{f_2^0}{\sqrt{3}} \end{pmatrix}. \quad (13)$$

The mixing of f_2 - f_2' is described as

$$f_2 = (f_2^8 \cos \theta_T - f_2^0 \sin \theta_T), \quad (14)$$

$$f_2' = (f_2^8 \sin \theta_T + f_2^0 \cos \theta_T), \quad (15)$$

and the results of $\theta_T = (27 \pm 1)^\circ$ is selected from PDG [29]. Following the same theory as given in Sec. II A, we derive the decay amplitudes for PT and PV channels, and they are listed in Tab. VII.

B. Numerical results of the $\chi_{cJ} \rightarrow PV$ decays

The neutral PV channels of the χ_{c1} and χ_{c2} decays, such as $\pi^0 \rho^0$ and $\eta \omega$, etc, are forbidden by C -parity conservation. Furthermore, the $\chi_{c2} \rightarrow PV$ decays are not only suppressed by helicity selection rule, but also suffer from G-parity or isospin/ U -spin conservation [26]. Although these processes lack experimental observations, we still provide phenomenological predictions under existing models. It is worth mentioning that many PV and PT processes are difficult to effectively constrain theoretically, so we only provide numerical predictions based on relevant experimental data from PDG [29]. Moreover, the experimental limits are significantly less than the theoretical non-perturbative parameters that need to be determined, and effective results cannot be obtained without additional constraints. So in the following contents, we will refer to the parameter ratios of PP and VV processes to limit the upper bounds of parameters, in order to obtain early prediction results.

For the $\chi_{c1} \rightarrow PV$ decays, only two modes of $\chi_{c1} \rightarrow K \bar{K}^*$ have been measured [29]. Their experimental data are listed in the second column of Tab. VIII. In these decays, relevant non-perturbative coefficients a_{21}^{PV} and b_1^{PV} lack effective experimental constraints. Referring to our results of $\chi_{cJ} \rightarrow PP, VV$, the constraints of $\frac{a_{21}^{PV}}{a_{11}^{PV}} \leq 45\%$ and $\frac{b_1^{PV}}{a_{11}^{PV}} \leq 55\%$ are imposed to obtain the predictions. The branching ratio predictions results of $\chi_{c1} \rightarrow PV$ via the SU(3) flavor symmetry are shown in the third column of Tab. VIII, while ones including the breaking results are presented

TABLE VII: The SU(3) symmetry and breaking amplitudes of $\chi_{cJ} \rightarrow PV$ and $\chi_{cJ} \rightarrow PT$

Decay modes	Symmetry amplitudes	Breaking amplitudes
$\chi_{cJ} \rightarrow \pi^+ \rho^- / \pi^+ a_2^-$	$2a_{1J}^{MM}$	$2b_J^{MM}$
$\chi_{cJ} \rightarrow \pi^- \rho^+ / \pi^- a_2^+$	$2a_{1J}^{MM}$	$2b_J^{MM}$
$\chi_{cJ} \rightarrow K^+ K^{*-} / K^- K_2^{*+}$	$2a_{1J}^{MM}$	$-b_J^{MM}$
$\chi_{cJ} \rightarrow K^- K^{*+} / K^- K_2^{*+}$	$2a_{1J}^{MM}$	$-b_J^{MM}$
$\chi_{cJ} \rightarrow K^0 \bar{K}^{*0} / K^0 \bar{K}_2^{*0}$	$2a_{1J}^{MM}$	$-b_J^{MM}$
$\chi_{cJ} \rightarrow \bar{K}^0 K^{*0} / \bar{K}^0 K_2^{*0}$	$2a_{1J}^{MM}$	$-b_J^{MM}$
$\chi_{cJ} \rightarrow \pi^0 \rho^0 / \pi^0 a_2^0$	$2a_{1J}^{MM}$	$2b_J^{MM}$
$\chi_{cJ} \rightarrow \eta_1 \omega_1 / \eta_1 f_2^0$	$2a_{1J}^{MM} + 6a_{2J}^{MM}$	0
$\chi_{cJ} \rightarrow \eta_1 \omega_8 / \eta_1 f_2^8$	0	$2\sqrt{2}b_J^{MM}$
$\chi_{cJ} \rightarrow \eta_8 \omega_1 / \eta_8 f_2^0$	0	$2\sqrt{2}b_J^{MM}$
$\chi_{cJ} \rightarrow \eta_8 \omega_8 / \eta_8 f_2^8$	$2a_{1J}^{MM}$	$-2b_J^{MM}$
$\chi_{cJ} \rightarrow \eta \phi / \eta f_2'$	$2a_{1J}^{MM} (\cos(\theta_P - \theta_{V/T})) + 6a_{2J}^{MM} \sin \theta_P \sin \theta_{V/T}$	$-2b_J^{MM} (\cos \theta_P \cos \theta_{V/T} + \sqrt{2} \sin(\theta_P + \theta_{V/T}))$
$\chi_{cJ} \rightarrow \eta \omega / \eta f_2$	$2a_{1J}^{MM} (-\sin(\theta_P - \theta_{V/T})) - 6a_{2J}^{MM} \sin \theta_P \cos \theta_{V/T}$	$-2b_J^{MM} (\cos \theta_P \sin \theta_{V/T} - \sqrt{2} \cos(\theta_P + \theta_{V/T}))$
$\chi_{cJ} \rightarrow \eta' \phi / \eta' f_2'$	$2a_{1J}^{MM} (\sin(\theta_P - \theta_{V/T})) - 6a_{2J}^{MM} \cos \theta_P \sin \theta_{V/T}$	$-2b_J^{MM} (\sin \theta_P \cos \theta_{V/T} - \sqrt{2} \cos(\theta_P + \theta_{V/T}))$
$\chi_{cJ} \rightarrow \eta' \omega / \eta' f_2$	$2a_{1J}^{MM} (\cos(\theta_P - \theta_{V/T})) + 6a_{2J}^{MM} \cos \theta_P \cos \theta_{V/T}$	$-2b_J^{MM} (\sin \theta_P \sin \theta_{V/T} - \sqrt{2} \sin(\theta_P + \theta_{V/T}))$

in the last column of Tab. VIII. From Tab. VIII, one can see that many errors of our predictions are quite large, since there are no other experimental data to constrain a_{21}^{PV} , b_1^{PV} and corresponding two phases.

For the $\chi_{c2} \rightarrow PV$ decays, three decay modes, $\chi_{c2} \rightarrow K^\pm K^{*\mp}, K^0 \bar{K}^{*0} + c.c., \pi^\pm \rho^\mp$ have been measured [29], and they are listed in the second column of Tab. IX. As given in the third column of IX, within the SU(3) flavor symmetry, and the constrained a_{12}^{PV} from $\mathcal{B}(\chi_{c2} \rightarrow K^\pm K^{*\mp}, K^0 \bar{K}^{*0} + c.c.)$ can not explain the experimental data of $\mathcal{B}(\chi_{c2} \rightarrow \pi^\pm \rho^\mp)$. Furthermore, with the SU(3) flavor symmetry, $\mathcal{B}(\chi_{c2} \rightarrow \pi^\pm \rho^\mp)$ is on the order of $\mathcal{O}(10^{-4})$, and $\mathcal{B}(\chi_{c2} \rightarrow \pi^0 \rho^0)$ is on the order of $\mathcal{O}(10^{-5})$. If considering the SU(3) flavor breaking, their allowed minimum values are down by an order of magnitude. This means that a large breaking effect is needed to explain the experimental data of $\mathcal{B}(\chi_{c2} \rightarrow \pi^\pm \rho^\mp)$.

If considering the SU(3) flavor breaking and setting $\frac{a_{22}^{PV}}{a_{12}^{PV}} \leq 45\%$ as well as $\frac{b_2^{PV}}{a_{12}^{PV}} \leq 80\%$, all three experimental data are explained at the same time. Noted that three experimental data can not be explained together when $\frac{b_2^{PV}}{a_{12}^{PV}} \leq 63\%$. The predictions including the breaking contributions are presented in the last column of Tab. IX. One can see that a_{12}^{PV} , b_2^{PV} and β_{2PV} are well constrained by three experimental data within 1σ error. Nevertheless, there is no any constraint on a_{22}^{PV} and α_{2PV} , which due to large error in some $\chi_{c2} \rightarrow PV$ decays. Some predicted results fail to exhibit the anticipated theoretical suppression, as this effect is obscured by substantial theoretical uncertainties.

TABLE VIII: The branching ratios for the $\chi_{c1} \rightarrow PV$ decays within 1σ error (in units of 10^{-3}).

	Exp. data [29]	Symmetry	Including breaking
$\mathcal{B}(\chi_{c1} \rightarrow \pi^\pm \rho^\mp)$...	1.12 ± 0.11	2.78 ± 2.65
$\mathcal{B}(\chi_{c1} \rightarrow \pi^0 \rho^0)$...	0.56 ± 0.05	1.39 ± 1.32
$\mathcal{B}(\chi_{c1} \rightarrow K^\pm K^{*\mp})$	1.21 ± 0.23	1.08 ± 0.10	1.08 ± 0.10
$\mathcal{B}(\chi_{c1} \rightarrow K^0 \bar{K}^{*0} + c.c.)$	1.03 ± 0.15	1.08 ± 0.10	1.08 ± 0.10
$\mathcal{B}(\chi_{c1} \rightarrow \eta \phi)$...	0.21 ± 0.17	0.40 ± 0.40
$\mathcal{B}(\chi_{c1} \rightarrow \eta \omega)$...	0.47 ± 0.34	1.16 ± 1.15
$\mathcal{B}(\chi_{c1} \rightarrow \eta' \phi)$...	0.64 ± 0.64	0.87 ± 0.87
$\mathcal{B}(\chi_{c1} \rightarrow \eta' \omega)$...	0.77 ± 0.77	1.93 ± 1.93
$a_{11}^{PV} (10^{-3})$...	4.68 ± 0.32	5.12 ± 1.65
$a_{21}^{PV} (10^{-3})$...	1.11 ± 1.11	1.46 ± 1.46
$b_1^{PV} (10^{-3})$	1.85 ± 1.85
$ \alpha_{1PV} $...	$(90.00 \pm 90.00)^\circ$	$(90.00 \pm 90.00)^\circ$
$ \beta_{1PV} $	$(90.00 \pm 90.00)^\circ$

TABLE IX: The branching ratios for the $\chi_{c2} \rightarrow PV$ decays within 1σ error (in units of 10^{-4}). #indicates that experimental data was not used to derive the numerical results.

	Exp. data [29]	Symmetry	Including breaking
$\mathcal{B}(\chi_{c2} \rightarrow \pi^\pm \rho^\mp)$	0.06 ± 0.04	$1.45 \pm 0.15^\#$	0.06 ± 0.04
$\mathcal{B}(\chi_{c2} \rightarrow \pi^0 \rho^0)$...	0.73 ± 0.08	0.03 ± 0.02
$\mathcal{B}(\chi_{c2} \rightarrow K^\pm K^{*\mp})$	1.46 ± 0.21	1.40 ± 0.15	1.40 ± 0.15
$\mathcal{B}(\chi_{c2} \rightarrow K^0 \bar{K}^{*0} + c.c.)$	1.27 ± 0.27	1.40 ± 0.15	1.40 ± 0.15
$\mathcal{B}(\chi_{c2} \rightarrow \eta \phi)$...	0.28 ± 0.23	0.91 ± 0.48
$\mathcal{B}(\chi_{c2} \rightarrow \eta \omega)$...	0.59 ± 0.43	0.09 ± 0.09
$\mathcal{B}(\chi_{c2} \rightarrow \eta' \phi)$...	0.81 ± 0.81	1.55 ± 1.25
$\mathcal{B}(\chi_{c2} \rightarrow \eta' \omega)$...	1.01 ± 1.01	0.31 ± 0.31
$a_{12}^{PV} (10^{-3})$...	2.60 ± 0.19	1.91 ± 0.18
$a_{22}^{PV} (10^{-3})$...	0.61 ± 0.61	0.46 ± 0.46
$b_2^{PV} (10^{-3})$	1.38 ± 0.21
$ \alpha_{2PV} $...	$(90.00 \pm 90.00)^\circ$	$(90.00 \pm 90.00)^\circ$
$ \beta_{2PV} $	$(169.60 \pm 10.31)^\circ$

And the branching ratios of $\chi_{c2} \rightarrow \pi \rho$ and $\chi_{c2} \rightarrow \eta \omega$ are significantly smaller compared to other decay channels when the flavor breaking effects are included. If we do not consider the theoretically forbidden scenario, this may be a signal that is suppressed by helicity selection rule or other theories.

Moreover, please noted that the predicted branching ratios of $K^\pm K^{*\mp}$ and $K^0 \bar{K}^{*0} + c.c.$ are completely consistent in both symmetry and breaking cases. The main reason is that their shared amplitude structure $2a_{1J}^{PV} - b_J^{PV} e^{i\beta_J^{PV}}$ and the effective constraints on $|2a_{1J}^{PV} - b_J^{PV} e^{i\beta_J^{PV}}|$ are actually obtained from the data of $K^\pm K^{*\mp}$ and $K^0 \bar{K}^{*0} + c.c.$ decays at present. The similar situation appear in the $\chi_{c1,2} \rightarrow PT$ decays.

C. Numerical results of the $\chi_{cJ} \rightarrow PT$ decays

For the PT decays, there are no C/G -parity conservation imposes prohibitive constraints, and helicity selection rule does not cause significant suppression. This theoretical landscape enables richer predictions for viable decay channels. Experimental measurements for $\chi_{c1} \rightarrow PT$ and $\chi_{c2} \rightarrow PT$ decays are compiled in the second columns of Tab. X and Tab. XI, respectively. SU(3) symmetry predictions occupy the third columns, and including breaking cases presented in the final columns.

TABLE X: The branching ratios for the $\chi_{c1} \rightarrow PT$ decays within 1σ error (in units of 10^{-3}).

	Exp. data [29]	Symmetry	Including breaking
$\mathcal{B}(\chi_{c1} \rightarrow \pi^\pm a_2^\mp)$...	1.42 ± 0.04	3.03 ± 2.14
$\mathcal{B}(\chi_{c1} \rightarrow \pi^0 a_2^0)$...	0.71 ± 0.02	1.51 ± 1.07
$\mathcal{B}(\chi_{c1} \rightarrow K^\pm K_2^{*\mp})$	1.61 ± 0.31	1.34 ± 0.04	1.34 ± 0.04
$\mathcal{B}(\chi_{c1} \rightarrow K^0 \bar{K}_2^{*0} + c.c.)$	1.17 ± 0.20	1.33 ± 0.04	1.33 ± 0.04
$\mathcal{B}(\chi_{c1} \rightarrow \eta f_2')$...	0.23 ± 0.03	0.42 ± 0.31
$\mathcal{B}(\chi_{c1} \rightarrow \eta f_2)$	0.67 ± 0.11	0.61 ± 0.05	0.67 ± 0.11
$\mathcal{B}(\chi_{c1} \rightarrow \eta' f_2')$...	0.60 ± 0.07	0.76 ± 0.76
$\mathcal{B}(\chi_{c1} \rightarrow \eta' f_2)$...	0.99 ± 0.21	1.49 ± 1.49
$a_{11}^{PT} (10^{-3})$...	5.54 ± 0.20	6.09 ± 1.16
$a_{21}^{PT} (10^{-3})$...	1.18 ± 0.25	1.60 ± 1.60
$b_1^{PT} (10^{-3})$	1.92 ± 1.92
$ \alpha_{1PT} $...	$(25.78 \pm 25.78)^\circ$	$(90.00 \pm 90.00)^\circ$
$ \beta_{1PT} $	$(90.00 \pm 90.00)^\circ$

TABLE XI: The branching ratios for the $\chi_{c2} \rightarrow PT$ decays within 1σ error (in units of 10^{-3}). # indicates that experimental data was not used to derive the numerical results.

	Exp. data [29]	Symmetry	Including breaking
$\mathcal{B}(\chi_{c2} \rightarrow \pi^\pm a_2^\mp)$	1.80 ± 0.60	1.50 ± 0.03	2.16 ± 0.24
$\mathcal{B}(\chi_{c2} \rightarrow \pi^0 a_2^0)$	1.31 ± 0.35	$0.75 \pm 0.02^\#$	1.08 ± 0.12
$\mathcal{B}(\chi_{c2} \rightarrow K^\pm K_2^{*\mp})$	1.51 ± 0.13	1.41 ± 0.03	1.41 ± 0.03
$\mathcal{B}(\chi_{c2} \rightarrow K^0 \bar{K}_2^{*0} + c.c.)$	1.27 ± 0.17	1.41 ± 0.03	1.41 ± 0.03
$\mathcal{B}(\chi_{c2} \rightarrow \eta f_2')$...	0.37 ± 0.15	0.45 ± 0.36
$\mathcal{B}(\chi_{c2} \rightarrow \eta f_2)$...	0.41 ± 0.25	0.77 ± 0.62
$\mathcal{B}(\chi_{c2} \rightarrow \eta' f_2')$...	0.37 ± 0.32	0.81 ± 0.81
$\mathcal{B}(\chi_{c2} \rightarrow \eta' f_2)$...	0.70 ± 0.70	1.59 ± 1.59
$a_{12}^{PT} (10^{-3})$...	8.77 ± 0.30	9.10 ± 0.70
$a_{22}^{PT} (10^{-3})$...	1.13 ± 1.13	2.19 ± 2.19
$b_2^{PT} (10^{-3})$	2.86 ± 2.14
$ \alpha_{2PT} $...	$(90.00 \pm 90.00)^\circ$	$(90.00 \pm 90.00)^\circ$
$ \beta_{2PT} $	$(43.54 \pm 43.54)^\circ$

The $\eta f'_2$, ηf_2 , $\eta' f'_2$ and $\eta' f_2$ channels exhibit sensitivity to the a_{2J}^{PT} amplitude parameter. However, the absence of experimental constraints make it difficult to determine the accuracy of a_{2J}^{PT} and b_J^{PT} in the simulation, especially there is no experimental data in $\chi_{c2} \rightarrow PT$ that can limit the range of a_{22}^{PT} . To address this, we impose the upper limits, $\frac{a_{2J}^{PT}}{a_{1J}^{PT}} \leq 45\%$ and $\frac{b_J^{PT}}{a_{1J}^{PT}} \leq 55\%$, based on analysis of PP and VV channels.

For the $\chi_{c1} \rightarrow PT$ decays, the ηf_2 channel provides critical constraints on a_{21}^{PT} and α_{1PT} , improving the accuracy of predicting $\eta f'_2$, $\eta' f'_2$ and $\eta' f_2$ channels in the SU(3) flavor symmetry case. After considering the SU(3) flavor breaking, a_{21}^{PT} and b_1^{PT} are not constrained well, and corresponding phase α_{1PT} and β_{1PT} are completely unrestricted. These bring about large errors in $\mathcal{B}(\chi_{c1} \rightarrow \pi^\pm a_2^\mp)$, $\mathcal{B}(\chi_{c1} \rightarrow \pi^0 a_2^0)$, $\mathcal{B}(\chi_{c1} \rightarrow \eta' f'_2)$ and $\mathcal{B}(\chi_{c1} \rightarrow \eta' f_2)$, and the measurements of these branching ratios could further constrained relevant non-perturbative coefficients.

For the $\chi_{c2} \rightarrow PT$ decays, in the SU(3) flavor symmetry case, the experiential data of $\mathcal{B}(\chi_{c2} \rightarrow \pi^\pm a_2^\mp)$, $\mathcal{B}(\chi_{c2} \rightarrow K^\pm K_2^{*\mp})$ and $\mathcal{B}(\chi_{c2} \rightarrow K^0 \bar{K}_2^{*0} + c.c.)$ give quite strong constraint on a_{12}^{PT} , and the data of $\mathcal{B}(\chi_{c2} \rightarrow \pi^0 a_2^0)$ can not be explained with other three ones together. Since there is no experimental constraint on a_{22}^{PT} and α_{2PT} , the sources of errors are increased and there are relatively large ranges of uncertainty in the $\chi_{c2} \rightarrow \eta f'_2$, ηf_2 , $\eta' f'_2$ and $\eta' f_2$ channels.

After considering the SU(3) flavor breaking, all four experimental data of the $\chi_{c2} \rightarrow PT$ decays can be explained together within 1σ error bar. And the current experimental data impose some restrictions on b_2^{PT} and β_{2PT} , but they are not strong. In fact, for all PV and PT processes, effective limitations have only been imposed on $a_{1J}^{PV,PT}$ within the existing experimental constraints, which at least ensures that all predicted results reflect the basic characteristics of the decay channels.

IV. CONCLUSION

Previous measurements by BESIII were based on the accumulated 448 million $\psi(3686)$ decays [40], which allowed access to χ_{cJ} decays through radiative decays $\psi(3686) \rightarrow \gamma \chi_{cJ}$. With a current data sample of 2.7 billion $\psi(3686)$ events collected by the BESIII detector [5], a more detailed analysis of two body χ_{cJ} decays is now possible. This provides an opportunity to test the SU(3) symmetry and gain deeper insights into their decay mechanisms.

In this work, we have investigated the $\chi_{c0,2} \rightarrow PP$, $\chi_{c0,1,2} \rightarrow VV$ and $\chi_{c1,2} \rightarrow PV, PT$ decays with the SU(3) flavor symmetry/breaking approach. We have obtained the amplitude relations in both SU(3) flavor symmetry case and further including SU(3) flavor breaking case. Because the advantages of symmetry approach, inconclusive intermediate decay mechanisms can be avoided from discussion. All branching ratios, including the predicted results for not-yet-measured or not-well-measured channels, have been presented in the work.

Our study shows that the SU(3) symmetry approach work well in the two body decays of charmonium states χ_{cJ} at present, which are typically difficult to compute using traditional QCD methods. Specifically, the $\chi_{cJ} \rightarrow \eta\eta'$ and $\chi_{cJ} \rightarrow \omega\phi$ are doubly OZI-suppressed, resulting in branching ratios for these decays are obviously smaller than those for the singly OZI-suppressed decays $\chi_{cJ} \rightarrow \eta\eta$, $\eta\eta'$, $\omega\omega$ and $\phi\phi$ [20, 35, 36, 41]. Our results are consistent with the suppression of the $\eta\eta'$ and $\omega\phi$ channels in the contributions of a_{2J}^M and align well with experimental data for these channels.

Our predictions not only contribute to future experimental measurements, but also offer valuable reference points for future theoretical works that aims to refine these calculations. Furthermore, with the high luminosity of the current experiments [42–44], we can expect a continuous stream of interesting experimental results to emerge, including precise

measurements of branching ratios and potentially new insights into the decay mechanisms of χ_{cJ} decaying into meson pairs.

ACKNOWLEDGEMENTS

The work was supported by the National Natural Science Foundation of China (Nos. 12175088, 12305100 and 12365014) and Graduate Innovation Fund Project of Jiangxi Provincial Department of Education (No. YJS2024091).

References

-
- [1] J. Z. Bai *et al.*, (BES), Phys. Lett. B **550**, 24-32 (2002)
 - [2] M. Ablikim *et al.*, (BESIII), Chin. Phys. C **37**, 063001 (2013)
 - [3] M. Ablikim *et al.*, (BESIII), Chin. Phys. C **37**, 123001 (2013)
 - [4] M. Ablikim *et al.*, (BESIII), Chin. Phys. C **42**, no.2, 023001 (2018)
 - [5] M. Ablikim *et al.*, (BESIII), Chin. Phys. C **48**, no.9, 093001 (2024)
 - [6] M. Ablikim *et al.*, (BES), Phys. Lett. B **630**, 7-13 (2005)
 - [7] A. V. Luchinsky, Phys. Atom. Nucl. **70**, 53-55 (2007)
 - [8] G. S. Adams *et al.*, (CLEO), Phys. Rev. D **75**, 071101 (2007)
 - [9] D. M. Asner *et al.*, (CLEO), Phys. Rev. D **79**, 072007 (2009)
 - [10] M. Ablikim *et al.*, (BESIII), Phys. Rev. D **81**, 052005 (2010)
 - [11] H. Chen and R. G. Ping, Phys. Rev. D **88**, 034025 (2013)
 - [12] F. Gross, *et al.*, Eur. Phys. J. C **83**, 1125 (2023)
 - [13] H. Y. Cheng and C. W. Chiang, Phys. Rev. D **81**, 074021 (2010)
 - [14] H. Y. Cheng and C. W. Chiang, Phys. Rev. D **85**, 034036 (2012) [erratum: Phys. Rev. D **85**, 079903 (2012)]
 - [15] J. Iizuka, Prog. Theor. Phys. Suppl. **37**, 21-34 (1966)
 - [16] Q. Zhao, Phys. Lett. B **659**, 221-227 (2008)
 - [17] C. E. Thomas, JHEP **10**, 026 (2007)
 - [18] D. Y. Chen, J. He, X. Q. Li and X. Liu, Phys. Rev. D **81**, 074006 (2010)
 - [19] M. Ablikim *et al.*, (BESIII), Phys. Rev. D **99**, 012015 (2019)
 - [20] M. Ablikim *et al.*, (BESII), Phys. Rev. Lett. **107**, 092001 (2011)
 - [21] Q. Wang, G. Li and Q. Zhao, Int. J. Mod. Phys. A **27**, 1250135 (2012)
 - [22] V. L. Chernyak and A. R. Zhitnitsky, Nucl. Phys. B **201**, 492 (1982) [erratum: Nucl. Phys. B **214**, 547 (1983)]
 - [23] W. E. Caswell and G. P. Lepage, Phys. Lett. B **167**, 437-442 (1986)
 - [24] N. Brambilla, A. Pineda, J. Soto and A. Vairo, Nucl. Phys. B **566**, 275 (2000)
 - [25] Q. Zhao, Phys. Rev. D **72**, 074001 (2005)
 - [26] X. H. Liu and Q. Zhao, Phys. Rev. D **81**, 014017 (2010)
 - [27] H. Q. Zhou, R. G. Ping and B. S. Zou, Phys. Lett. B **611**, 123-128 (2005)
 - [28] N. Kivel, JHEP **07**, 065 (2024)
 - [29] S. Navas *et al.*, (Particle Data Group), Phys. Rev. D **110**, 030001 (2024)

- [30] M. Gronau, O. F. Hernandez, D. London and J. L. Rosner, Phys. Rev. D **52**, 6356-6373 (1995)
 - [31] D. Xu, G. N. Li and X. G. He, Int. J. Mod. Phys. A **29**, 1450011 (2014)
 - [32] X. G. He, G. N. Li and D. Xu, Phys. Rev. D **91**, 014029 (2015)
 - [33] M. Gronau, O. F. Hernandez, D. London and J. L. Rosner, Phys. Rev. D **50**, 4529-4543 (1994)
 - [34] D. Wang, C. P. Jia and F. S. Yu, JHEP **21**, 126 (2020)
 - [35] M. Ablikim *et al.*, (BESIII), Phys. Rev. D **96**, 112006 (2017)
 - [36] B. Zheng (BESIII), PoS **Hadron2017**, 096 (2018)
 - [37] M. Ablikim *et al.*, (BESIII), arXiv:2502.08929 [hep-ex]
 - [38] R. Aaij *et al.*, (LHCb), Phys. Rev. D **108**, 032010 (2023)
 - [39] M. Ablikim *et al.*, (BES), Phys. Rev. D **74**, 072001 (2006)
 - [40] M. Ablikim *et al.*, (BESIII), Chin. Phys. C **44**, 040001 (2020)
 - [41] M. N. Achasov *et al.*, Phys. Usp. **1**, 55-70 (2024)
 - [42] A. E. Bondar *et al.*, (Charm-Tau Factory), Phys. Atom. Nucl. **76**, 1072-1085 (2013)
 - [43] H. P. Peng, Y. H. Zheng and X. R. Zhou, Physics **49**, 513-524 (2020)
 - [44] M. Ablikim *et al.*, (BESIII), Chin. Phys. C **48**, 123001 (2024)
-